International Journal of Smart Home
Vol.7, No.5 (2013), pp.173-186
http://dx.doi.org/10.14257/ijsh.2013.7.5.18

An Offline Current-Mode PFM Controller for Low Power Residential LED Lighting with Primary-Side Constant Current Regulation Techniques

Yong-Rui Zhao[1] and Xin-Quan Lai[2]

[1] *Institute of Electronic CAD, Xidian University, Xi'an, Shaanxi 710071, China*
[2] *Key Lab of High-Speed Circuit Design and EMC, Ministry of Education, Xidian University, Xi'an, Shaanxi 710071, China*
[1] *yrzhao@mail.xidian.edu.cn,* [2] *xqlai@mail.xidian.edu.cn*

Abstract

This paper presents an offline current-mode pulse frequency modulation (PFM) controller for low power residential LED lighting, which has a better performance and a simplified structure. A novel controller which contains Constant Current (CC) regulation technique based on auxiliary winding feedback and pulse frequency modulation (PFM) mode basing on the flyback structure is presented, which simplifies the application environment. Also, an input power adjusting technique is introduced which improves the working stability. These techniques are validated by using an integrated circuit designed in 0.5-μm 700V BCD process. In the constant area, when the input AC voltage is from 85V-220V and the load resistance is from 3Ω to 4.7Ω, the test results of actual application circuit show the constant current point is about 1A and the current ripple is about ±4%.

Keywords: *LED lighting; flyback; Constant Current control; PFM*

1. Introduction

With the wide application of electronic products, people's requirements on the power supplies become more and more strict. For example, the LED drivers need constant current, and the lithium battery charger needs constant current and constant voltage. AC-DC converters [1] which change AC into DC by the use of semiconductor devices can meet these requirements. The topology of flyback [2, 3] has been widely used in the AC-DC converters due to the facts that it provides input-output isolation and the number of its semiconductor and magnetic components is less than other switching power supplies.

Flyback converter can operate in pulse frequency modulation (PFM) mode [4-6], pulse width modulation (PWM) mode [7-9] and pulse skip modulation (PSM) mode. In order to improve efficiency, most AC-DC converters work in PWM mode on the heavy load (constant current) state, and in PFM mode or PSM mode on the light load (constant voltage) state. To achieve the purpose of constant current, most AC-DC converters operate in PFM mode or PWM mode. Compared with PWM mode, PFM mode can make the system application circuit achieve higher efficiency. When the esternal circuits of PWM mode are same as those of PFM mode, these circuits will have the same peak efficiency. But before getting the point of peak power, the efficiency of the circuits which are controlled by PFM mode is much higher than those controlled by PWM mode. What's more, the PWM controller will be affected by

ISSN: 1975-4094 IJSH

error amplifier and loop gain as well as response speed, the circuits controlled by PFM mode have a faster response speed than those controlled by PWM mode. Nowadays, to achieve the purpose of the constant current, most AC-DC converters need the help of secondary loop control circuit and optocoupler, the system application circuit becomes complex and its cost is high. Based on the above factors, in order to achieve the purpose of constant current on the premise of removing the optocoupler and secondary loop control circuit, a new type CC (constant current) control circuit based on auxiliary winding feedback and PFM mode was proposed, which greatly simplifies the application circuit and reduces the overall cost. In the constant region, when the load changes, the circuit proposed in this paper will change the system working frequency to adjust the input power, then it can achieve the purpose of constant current. The constant current control circuit is used in a 5V/1A Constant Current (CC) and Constant Voltage (CV) AC-DC converter. The AC-DC converter was fabricated in a 0.5-μm BCD process [10] with an area of. Experimental results prove the AC-DC converter can get the constant current of 1A when the input voltage and the load resistance change.

2. Method Description

Since the traditional offline isolation LED lighting methods always use signals feedbacking from the secondary side of the transformer, as shown in reference [5, 11] and [12], a complex application environment is needed for improving the cost of the whole circuit and blocking the widely use of the green lighting. Consequently, the primary-side PFM constant current control methods are introduced, which are shown below.

The circuit proposed in this paper is applied in a 5V/1A CV/CC AC-DC converter which is based on flyback topology. The system architecture is shown in Figure 1.

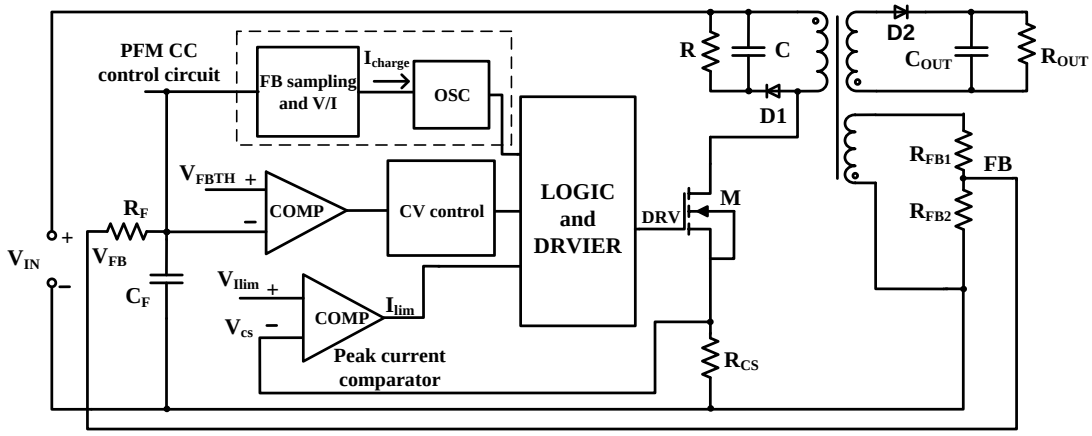

Figure 1. System Architecture Diagram

Initially, the output voltage is low, so the sampling voltage of the FB pin is not high, and the voltage is less than V_{FBTH}. Thus, the CV control circuit does not work, and the PFM CC control circuit operates in normal state. The continuous opening and closing of the switching MOS device keep the output voltage rising. In the CC region, the feedback voltage of FB pin will not exceed V_{FBTH}, so the CV control circuit won't work.Changes in the output load will alter the sampled FB voltage, thus the changing of V_{FB} affects the operating frequency of the switching power MOSFET, and then the switching frequency increases as the FB voltage increases to adjust the size of the input power and provide constant output current regulation. As the FB approaches V_{FBTH} , the

system begins to work in CV mode. At this point, system gets the peak power point of CC/CV characteristic and the switching frequency of CV mode is at its maximum value The CV control circuit regulates the FB voltage to remain at V_{FBTH}, and the FB voltage is sampled 2.5μs after the turn-off of the high voltage switch.

In the CC region, the maximum conduction duty and switching frequency of this AC-DC converter is controlled by the internal oscillator, while the reasonable settings of the value of peripheral devices can make the converter only work in discontinuous conduction mode (DCM) [11, 12]. In a switching period, the primary coil energy has all been passed to the output stage. When the power MOSFET is on, the main secondary coil has no disturbance current of the feedback by the secondary coil, so the slope compensation circuit commonly used in the PWM controller is not required, and this can save the layout area.

The primary coil current waveforms of flyback converter in DCM as shown below:

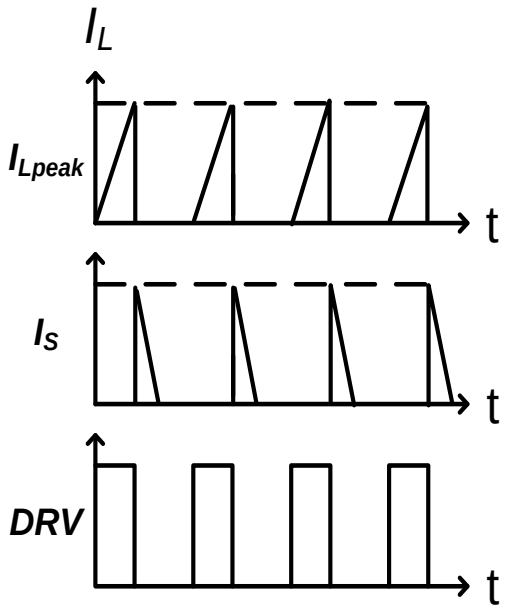

Figure 2. The Waveforms of Flyback Converter in DCM Mode

When the power MOSFET is on, the primary inductor current ramps up from zero by a slope of V_{IN}/L. Where V_{IN} is the DC voltage after rectification and filtration of AC input, and L is the value of primary inductor. As the result of the peak current control mode, the power MOSFET is turned off after the primary inductor current rises to the limited $I_{Lpeak}=V_{CS}/R_{CS}$. Where V_{Ilim} is the current limit voltage of peak current comparator, R_{cs} is the current sense resistor.

At this point, the energy stored in the transformer is:

$$E = \frac{1}{2} L(I_{Lpeak})^2 = \frac{1}{2} L(\frac{V_{I_{\lim}}}{R_{CS}})^2 \quad (1)$$

In DCM mode, the secondary inductor current I_S has dropped to zero before the power MOSFET conducts again, so the energy stored in the transformer has been all sent to the output load in a switching cycle. Then output power which is provided by the input is

$$P_{out} = V_{out} \times I_{out} = \eta \frac{L(I_{Lpeak})^2}{2} f = \eta \frac{L}{2} f (\frac{V_{I_{\lim}}}{R_{CS}})^2 \quad (2)$$

In the equation above, η is the efficiency of the flyback transformer, V_{out} is the output voltage, I_{out} is the output current. V_{Ilim}, R_{CS} , L are fixed values. It can be seen, for a fixed external circuit, the system output power is only proportional to the frequency.

During the time when the secondary coil release the energy, we can get from figure 1 that

$$V_{out} = \frac{N_S}{N_A} \frac{R_{FB1} + R_{FB2}}{R_{FB2}} V_{FB} = KV_{FB} \quad (3)$$

where, $K = \frac{N_S}{N_A} \frac{R_{FB1} + R_{FB2}}{R_{FB2}}$, K is a constant value, NS is auxiliary winding turns of the flyback converter, N_A is the secondary coil turns, R_{FB1} and R_{FB2} are voltage dividers.

From the equation (2) and (3), the output current is

$$I_{out} = \eta \frac{L(I_{Lpeak})^2}{2Vout} f = \eta \frac{L}{2} \frac{f}{KV_{FB}Vout} (\frac{V_{I_{\lim}}}{R_{CS}})^2 \quad (4)$$

where, let $K' = \eta \frac{L}{2} \frac{1}{K} (\frac{V_{I_{\lim}}}{R_{CS}})^2$, K' is a constant value, so the equation can be simplified as

$$I_{out} = K' \frac{f}{V_{FB}} \quad (5)$$

It can been seen from the above equation that if there is a linear relationship between f and V_{FB}, the output current I_{out} will be a constant value.

3. The Design of PFM CC Control Circuit

If all the other parameters are fixed, we can know through the above analysis that the frequency of the system is only controlled by V_{FB}, the output current is kept constant in the constant current region. Therefore, according to such circumstances, a V/I converting circuit shown in Figure 3 and the oscillator circuit shown in Figure 4 have been designed in this paper. In the CC region, the sampled FB voltage will be changed with the different output loads. Figure 3 shows the influence of FB voltage on the oscillator operating current I_{charge}, the oscillator frequency is proportional to the size of I_{charge}, and the system operating frequency is decided by the oscillator. Therefore, changes in the load will alter the operating frequency of the power MOSFET to adjust the input power to achieve the purpose of CC.

3.1. V/I Converting Circuit

It can be seen from the system architecture diagram shown in Figure 1 that FB pin voltage is got through a resistor divider of auxiliary winding. The power MOSFET is turned on and off constantly, so the FB voltage is not a linear changing value. When the power MOSFET is on, the FB voltage is very low, and during the shutdown period, the FB pin senses the output voltage before the secondary inductance energy decrease to zero. When there is no energy in the secondary inductor, oscillation will occur due to the primary inductance and the parasitic capacitance of the power MOSFET. In order to let FB pin voltage make the correct response to the output voltage, a sampling and holding circuit of FB voltage is designed and shown in the left part of Figure 3. The high frequency noise of FB pin has been removed by the low pass filter which is made up of resistor R5 and capacitor C2. When the power MOSFET is turned off 2.5 μs later, there will be a high pulse signal S_Delay on the gate of M12, so the M12 is turned on and a current through the M12 charges the capacitor C1. But S_Delay becomes low soon, and the voltage of C1 remains until the arrival of the next pulse.

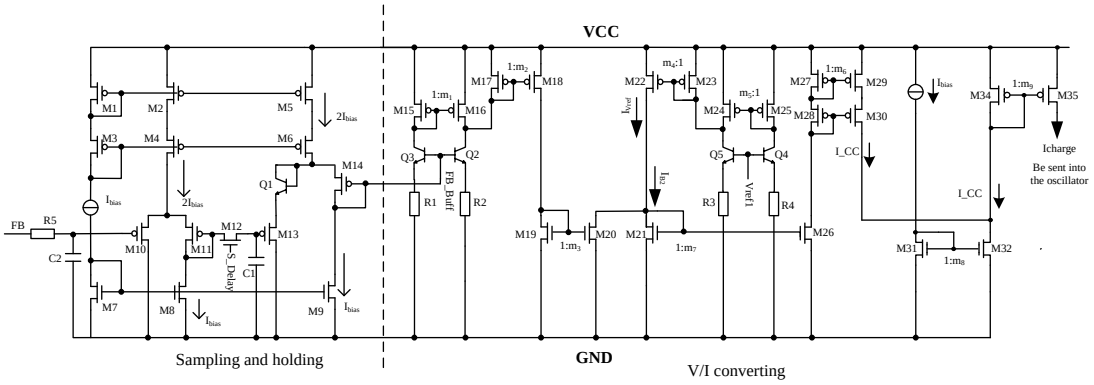

Figure 3.V/I Conversion Circuit

Current mirror relationship makes the current passing through M10 equal to that of M11, and the current of M13 equal to that of M14. Ignoring the channel modulation effect, and for the PMOS transistor in the saturated zone, there is

$$V_{SG} = V_{THP} + \sqrt{\frac{2I_D}{K}} \tag{6}$$

where V_{THP} and $K = \mu_p C_{ox} \frac{W}{L}$ are the threshold voltage and transconductance factor of PMOS. Because $(W/L)_{10}=(W/L)_{11}$, $(W/L)_{13}=(W/L)_{14}$, $V_{SG10}=V_{SG11}$, $V_{SG13}= V_{SG14}$. There comes a high pulse to make M12 be turned on, and a current charges the capacitor C1. The sampled voltage of FB pin is given by

$$V_{C1} = V_{FB} + V_{SG10} - V_{SG11} \tag{7}$$

where V_{FB} is the sampled voltage of FB pin. So the voltage of net FB_Buff is

$$\begin{aligned} V_{FB\_Buff} &= V_{C1} + V_{SG13} + V_{BE} - V_{SG14} = V_{FB} + V_{SG10} - V_{SG11} + V_{SG13} + V_{BE1} - V_{SG14} \\ &= V_{FB} + V_{BE1} \end{aligned} \tag{8}$$

M12 is turned off when S_Delay becomes low, and the voltage of C1 remains. So V_{FB_Buff} does not change until the coming of the next pulse. Net FB_Buff is connected to the base electrode of Q2 and Q3, thus two emitter followers are formed with these two NPN triodes. Because the input resistance of the emitter follower is very large, so the emitter voltage of Q2 and Q3 can well linearly change with V_{FB_Buff}. We can see from the Figure 3 that M15~M18 constitute a current mirror and subtraction circuit. The current in M18 is given by

$$I_{M_{18}} = m_2(\frac{V_{FB}+V_{BE1}-V_{BE2}}{R_2} - m_1\frac{V_{FB1}+V_{BE1}-V_{BE2}}{R_1}) \approx m_2 V_{FB}(\frac{1}{R_2} - m_1\frac{1}{R_1}) \quad (9)$$

where $(W/L)_{16}/(W/L)_{15}=m_1$, $(W/L)_{18}/(W/L)_{17}=m_2$.

Similarly, the current in M22 can be expressed as below

$$I_{M22} = (V_{ref1} - V_{BE})(\frac{1}{R_3} - \frac{m_5}{R_4})m_4 = V_{ref}(\frac{1}{R_3} - \frac{m_5}{R_4})m_4 \quad (10)$$

where $(W/L)_{24}/(W/L)_{25}=m_5$, $(W/L)_{22}/(W/L)_{23}=m_4$, and $V_{ref}=1.25V$, V_{ref} is the reference voltage of the converter. The current which flows into M32 from M29 and M30 is given by

$$\begin{aligned} I_{M30} &= m_6 m_7(I_{M22} - m_3 I_{M18}) = m_6 m_7(V_{ref}(\frac{1}{R_3} - \frac{m_5}{R_4})m_4 - m_2 m_3 V_{FB}(\frac{1}{R_2} - m_1\frac{1}{R_1})) \\ &= m_4 m_6 m_7 V_{ref}(\frac{1}{R_3} - \frac{m_5}{R_4}) - m_2 m_3 m_6 m_7 V_{FB}(\frac{1}{R_2} - m_1\frac{1}{R_1}) \end{aligned} \quad (11)$$

where $(W/L)_{20}=(W/L)_{19}=m_3$, $(W/L)_{29}/(W/L)_{27}=m_6$, $(W/L)_{26}/(W/L)_{21}=m_7$.

From the right part of figure 3, according to the relationship of current mirror and subtraction, we can get the output current which is sent into the oscillator as its charging and discharging current to control the frequency. The current is

$$I_{charge} = (m_8 I_{bias1} - I_{M30})m_9 \quad (12)$$

where $(W/L)_{32}/(W/L)_{31}=m_8$, $(W/L)_{35}/(W/L)_{34}=m_9$。

Taking equation （11） into （12）, a new equation can be got as

$$I_{charge} = m_8 m_9 I_{bias} + m_2 m_3 m_6 m_7 m_9 V_{FB}(\frac{1}{R_2} - m_1\frac{1}{R_1}) - m_4 m_6 m_7 m_9 V_{ref}(\frac{1}{R_3} - \frac{m_5}{R_4}) \quad (13)$$

where I_{bias} is the bias current of the converter. It is obvious from the equation (10) that the structure of current-subtraction can compensate the size of current caused by temperature, because the changing of temperature can alter resistance of the resistors in the circuit.

Let $\alpha_1 = m_8 m_9$, $\alpha_2 = m_2 m_3 m_6 m_7(\frac{1}{R_2} - m_1\frac{1}{R_1})$, $\alpha_3 = m_4 m_6 m_7(\frac{1}{R_3} - \frac{m_5}{R_4})$,and α_1, α_2, α_3 are all constant value. Using $\alpha_1 \sim \alpha_3$, equation （13） can be simplified as below

$$I_{charge} = \alpha_1 I_{bias} + \alpha_2 V_{FB} - \alpha_3 V_{ref} \tag{14}$$

3.2. Design of the Oscillator

As is shown in Figure 4, the proposed circuit is the relaxation oscillator [13-15] which can control its frequency by charging and discharging the capacitor. At the initial time, it can be assumed that the voltage of capacitor C is zero, the switching control signal XA makes the two top switches close, a current I_{charge} charges the capacitor C, when the voltage of C exceeds the threshold V1, the output of COMP1 generates a high level signal A to make the two switches below in the figure 4 close. The COMP2 operates normally, then, XA becomes low and make the two top switches close, and COMP1 doesn't work. The capacitor C begin to discharge and the discharge current is αI_{charge}, when the voltage of capacitor C is less than V2, a low level signal A comes from the output of

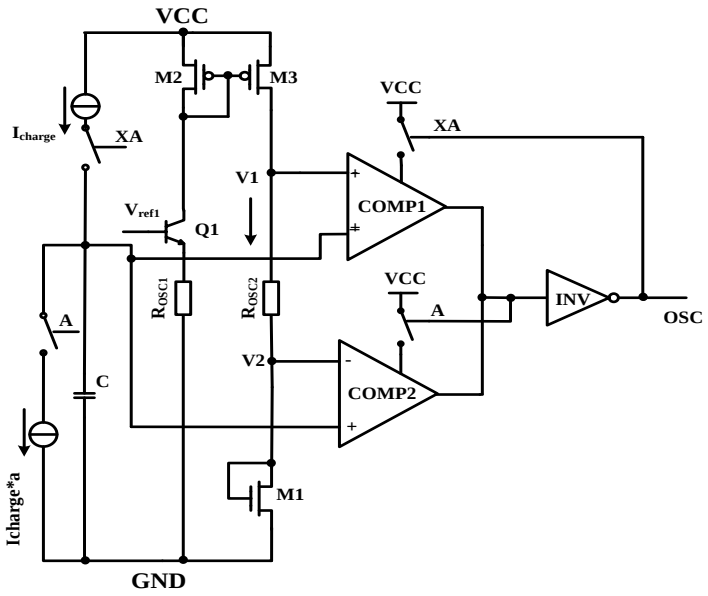

Figure 4. The Oscillator Circuit

COMP2, and XA becomes high. So the two top switches are closed and the other two are turned off. Thus, COMP1 operates normally and COMP2 doesn't work, and the oscillator enters the charging phase again. According to the above analysis of the working process, the charging time and discharging time form a cycle.

The charging time of capacitor C is

$$t_1 = \frac{(V2 - V1)C}{I_{charge}} = \frac{I_{M3} R_{osc2} C}{I_{charge}} \tag{15}$$

Because $(W/L)_2/(W/L)_3$=1, there is

$$I_{M3} = I_{M2} = \frac{V_{ref1} - V_{BE1}}{R_{OSC1}} = \frac{V_{ref}}{R_{OSC1}} \tag{16}$$

Taking equation (16) into equation (15), the charging time can be expressed as below

$$t_1 = \frac{R_{OSC2} C V_{ref}}{R_{OSC1} I_{charge}} \tag{17}$$

Similarly, the discharging time is given by

$$t_2 = \frac{R_{OSC2} C V_{ref}}{R_{OSC1} \alpha I_{charge}} \tag{18}$$

So the frequency of the oscillator is

$$f = \frac{1}{t_1 + t_2} = \frac{1}{\frac{R_{OSC2} C V_{ref}}{R_{OSC1} \alpha I_{charge}} + \frac{R_{OSC2} C V_{ref}}{R_{OSC1} I_{charge}}} = \frac{R_{OSC1} I_{charge}}{R_{OSC2} C V_{ref}} \frac{\alpha}{1+\alpha} \tag{19}$$

We can know that I_{charge} is proportional to the working frequency from the above equation (19), constant α controls the duty cycle of clock signal. Using the equation (19), a new equation got from the equation (14) is

$$f = \frac{R_{OSC1}(\alpha_1 I_{bias} + \alpha_2 V_{FB} - \alpha_3 V_{ref})}{R_{OSC2} C V_{ref}} \frac{\alpha}{1+\alpha} \tag{20}$$

where, $\frac{\partial f}{\partial V_{FB}} = \frac{\alpha}{1+\alpha} \frac{R_{OSC1} \alpha_2}{R_{OSC2} C V_{ref}}$. So it can be seen from this that system operating frequency changes linearly along V_{FB}.

4. Setting of Constant Current Point

Let $K_1 = \frac{R_{OSC1}(\alpha_1 I_{bias} - \alpha_3 V_{ref})}{R_{OSC2} C V_{ref}} \frac{\alpha}{1+\alpha}$, $K_2 = \frac{R_{OSC1} \alpha_2}{R_{OSC2} C V_{ref}} \frac{\alpha}{1+\alpha}$, where K_1 and K_2 are constant value, the equation (20) can be simplified as below

$$f = K_1 + K_2 V_{FB} \tag{21}$$

Using the equation (21) and (5), in the constant current phase, the output current is

$$I_{out} = K' \frac{K_1 + K_2 V_{FB}}{V_{FB}} \tag{22}$$

As the system begins to work, V_{FB} is almost equal to 0. In order to let the power MOSFET operate normally, so it must ensure that there is an initial frequency and the initial frequency is set to be a smaller value. When the output voltage increases, V_{FB} becomes larger. The contribution of K_1 to the system frequency can be neglected compared to V_{FB}. So when V_{FB} is a larger value, $f \approx K_2 V_{FB}$, the equation (22) can be simplified as

$$I_{out} = K^{'} K_2 \tag{23}$$

It can be seen from the above equation that when the feedback voltage is greater than a certain value, the converter can adjust the operating frequency to achieve the purpose of constant current with the changing of the output load.

5. Experimental Results

The proposed circuit in this paper is applied in the 5V/1A CV/CC AC-DC converter which is based on flyback structure, and its constant current operating point is 1A. This AC-DC converter has been designed and taped out by using the 700V BCD process. Figures 5-16 are tests results of the actual application circuit. When the input AC voltage is from 85V-220V and the load resistances are 3Ω, 4Ω, 4.7Ω, these 12 figures are shown as below.

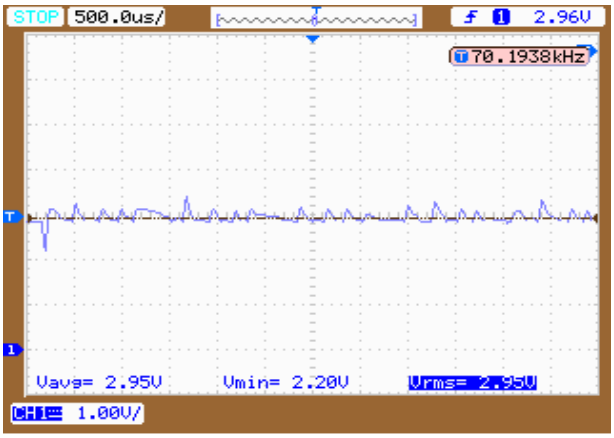

Figure 5. The Waveform of Output Voltage (3Ω, 85V)

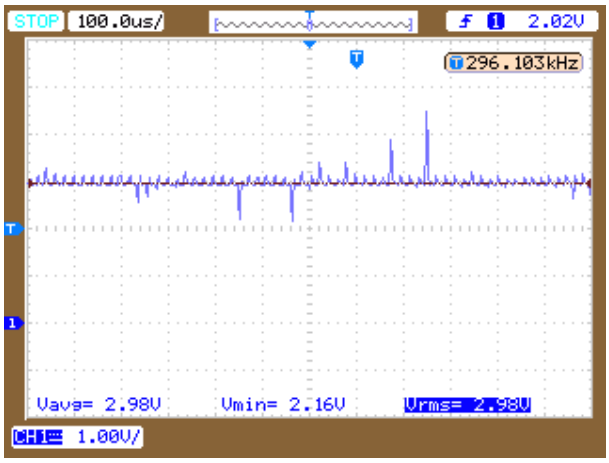

Figure 6. The Waveform of Output Voltage (3Ω, 110V)

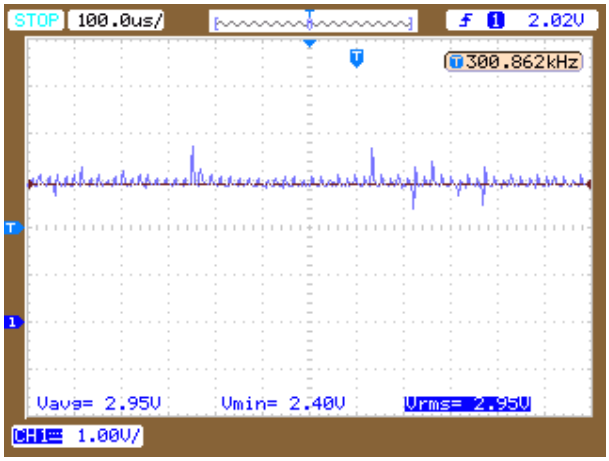

Figure 7. The Waveform of Output Voltage (3Ω, 220V)

We can see from Figures 5-7 that when the output resistance is 3Ω and the input voltage changes from 85-220V, the output current almost has no change, and it is about 993mA, and the current ripple is about ±4%.

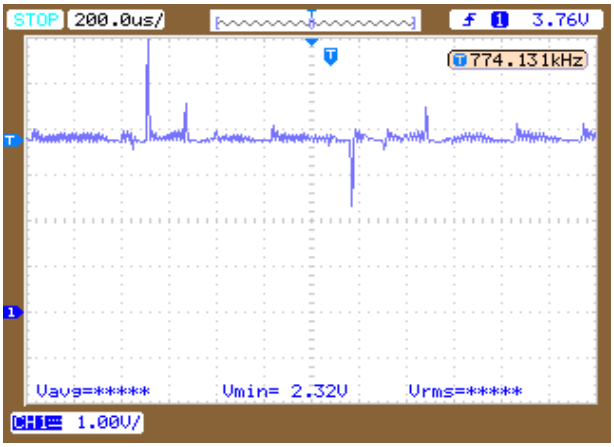

Figure 8. The Waveform of Output Voltage (4Ω, 85V)

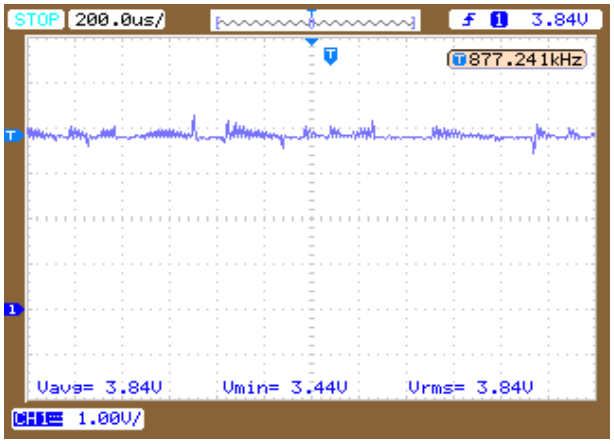

Figure 9. The Waveform of Output Voltage (4Ω, 110V)

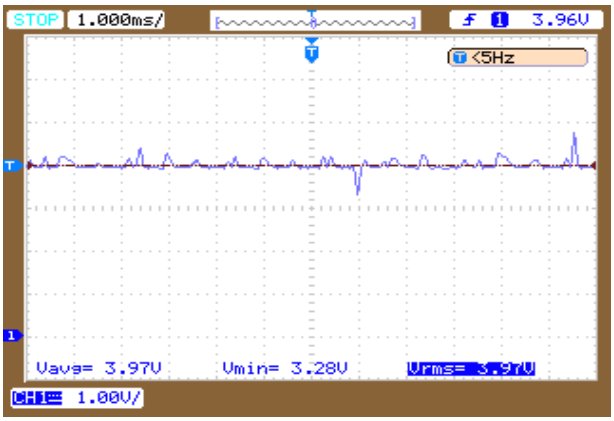

Figure 10. The Waveform of Output Voltage (4Ω, 220V)

Figures 8-10 are the waveforms of output voltage when the output resistance is 4Ω. It can be seen from these three figures that the output current is about 962mA when the input voltage is 85V and 110V, and when the input voltage is 220V, the output current is 992mA. But the output current ripple is about ±4%.

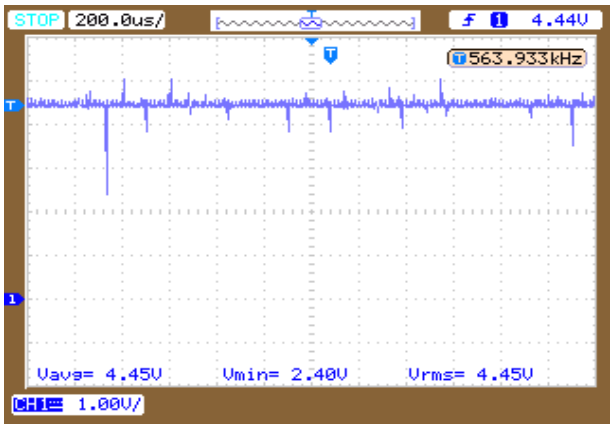

Figure 11. The Waveform of Output Voltage (4.7Ω, 85V)

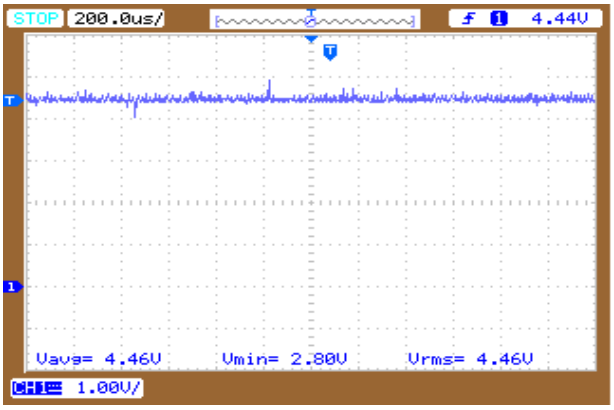

Figure 12. The Waveform of Output Voltage (4.7Ω, 110V)

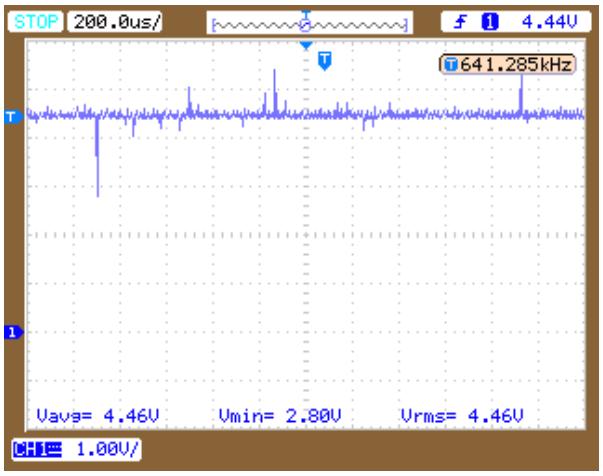

Figure 13. The Waveform of Output Voltage (4.7Ω, 220V)

It is obvious from Figures 11-13 that when the load resistance is 4.7Ω, the output current is about 948mA and its ripple is about ±4%.

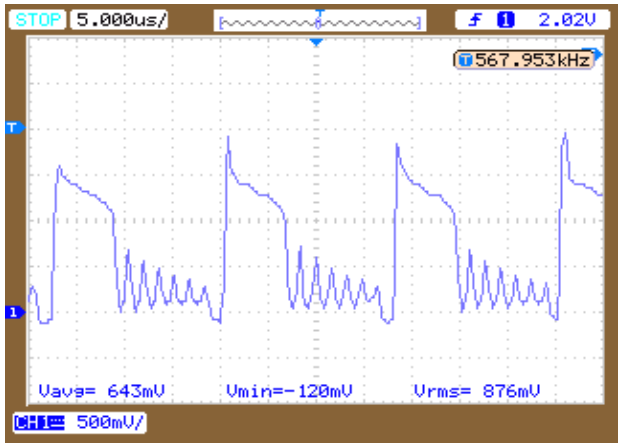

Figure 14. The Voltage Signal of FB Pin (3Ω)

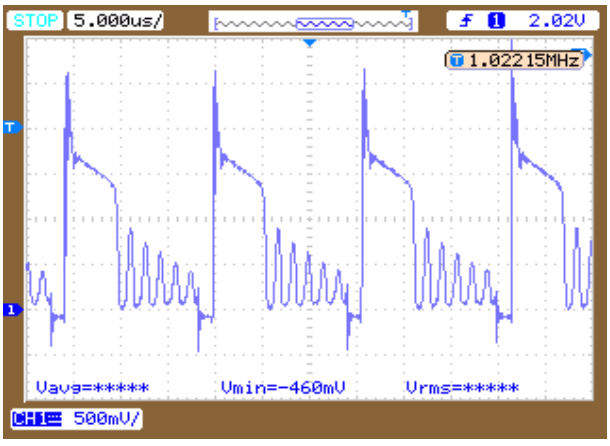

Figure 15. The Voltage Signal of FB Pin (4Ω)

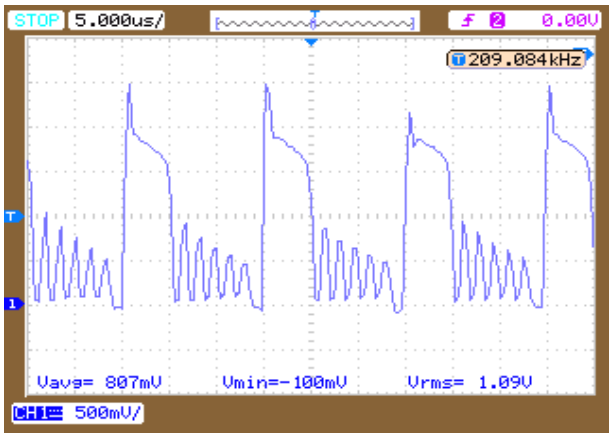

Figure 16. The Voltage Signal of FB Pin (4.7Ω)

In the CC region, the frequency of the voltage signal on FB pin is equal to the operating frequency of the system. So it can be seen in Figure14-16 that when the output resistance are 3Ω, 4Ω, 4.7Ω, the corresponding system working frequency are 55.5 KHz, 62.5 KHz and 66.6 KHz. So there is essentially a linear relationship between the system operating frequency and the size of load resistance.

According to the test results above, in the CC region, it is obvious that when the load resistance is changed from 3Ω to 4.7Ω, the output current keeps constant and the point of CC is about 1A. The chip can change its frequency with different loads to adjust input power to get the purpose of CC.

6. Conclusion

This paper is based on the principle of AC-DC converter which has the structure of flyback. In order to remove the optocoupler and secondary-loop control circuit, a novel PFM CC control circuit which is based on the auxiliary winding flyback was proposed in this paper. According to the test waveforms of the application circuit, the purpose of CC 1A had been achieved by the use of this PFM control circuit, what's more, the output current ripple of the application circuit is about only ±4%. This circuit can change the system frequency with different loads to adjust input power to achieve the purpose of CC. The circuit will greatly simplify the system application circuit and save the cost to make the AC-DC converter have a higher performance price ration compared to other converters.

Acknowledgements

This work was partly supported by Key Lab of High-Speed Circuit Design and EMC, Ministry of Education, the Xidian University of China (No.JY0100092702), and by a research granted by the National Natural Science Foundation of China (No. 61106026).

References

[1] S. Norrga, "Experimental Study of a Soft-Switched Isolated Bidirectional AC-DC converter Without Auxiliary Circuit", IEEE Transactions on Power Electronics, vol. 21, no. 6, **(2006)**, pp. 1580-1587.
[2] H. Chen, M.-L. Zhao, X.-B. Wu and X.-L. Yan, "Multi-mode controller IC for soft-switched flyback converter with high efficiency over the entire load range", Journal of Zhejiang University Science A, vol. 9, no. 10, **(2008)**, pp. 1411-1419.

[3] A. Hren, J. Korelic and M. Milanovic, "RC-RCD Clamp Circuit for Ringing Losses Reduction in a Flyback Converter", IEEE Transactions on Circuits and Systems II, vol. 53, no. 5, **(2006)**, pp. 369-373.
[4] Y. Chen and Y. Kang, "A Fully Regulated Dual-Output DC-DC Converter with Special-Connected Two Transformers (SCCTs) Cell and Complementary Pulsewidth Modulation-PFM (CPWM-PFM)", IEEE Transactions on Power Electronics, vol. 25, no. 5, **(2010)**, pp. 1296-1309.
[5] B. Sahu and G. A. Rincon-Mora, "An Accurate, Low-Voltage, CMOS Switching Power Supply With Adaptive On-Time Pulse-Frequency Modulation (PFM) Control", IEEE Transactions on Circuits and Systems I, vol. 54, no. 2, **(2007)**, pp. 312-321.
[6] Y.-S. Shin, C.-S. Kim and S.-K. Han, "A Pulse-Frequency-Modulated Full-Bridge DC/DC Converter with Series Boost Capacitor", IEEE Transactions on Industrial Electronics, vol. 58, no. 11, **(2011)**, pp. 5154-5162.
[7] Y. Chen and Y. Kang, "An Improved Full-Bridge Dual-Output DC-DC Converter Based on the Extended Complementary Pulsewidth Modulation Concept", IEEE Transactions on Power Electronics, vol. 26, no. 11, **(2011)**, pp. 3215-3229.
[8] Y. Suh and T. A. Liop, "Modeling and analysis of instantaneous active and reactive power for PWM AC/DC converter under generalized unbalanced network", IEEE Transactions on Power Delivery, vol. 21, no. 3, **(2006)**, pp. 1530-1540.
[9] L.-S. Yang, T.-J. Liang and J.-F. Chen, "Analysis and Design of a Novel Three-Phase AC-DC Buck-Boost Converter", IEEE Transactions on Power Electronics, vol. 23, no. 2, **(2008)**, pp. 707-714.
[10] S.-Fu Hsu and M.-D. Ker, "Dependence of Device Structures on Latchup Immunity in a High-Voltage 40-V CMOS Process with Drain-Extended MOSFETS", IEEE transactions on Electron Devices, vol. 54, no. 5, **(2007)**, pp. 840-851.
[11] J. A. Abu Qahouq, "Control Scheme for Sensorless Operation and Detection of CCM and DCM operation Modes in Synchronous Switching Power Converters", IEEE Transactions on Power Electronics, vol. 25, no. 10, **(2010)**, pp. 2489-2495.
[12] K. Yao, X. Ruan, X. Mao and Z. Ye, "Variable-Duty-Cycle Control to Achieve High Input Power Factor for DCM Boost PFC Converter", IEEE Transactions on Industrial Electronics, vol. 58, no. 5, **(2011)**, pp. 1856-1965.
[13] U. Denier, "Analysis and Design of an Ultralow-Power CMOS Relaxation Oscillator", IEEE Transactions on Circuits and Systems I, vol. 57, no. 8, **(2010)**, pp. 1973-1982.
[14] Y. Tokunaga, S. Sakiyama, A. Matsumoto and S. Dosho, "An On-Chip CMOS Relaxation Oscillator With Voltage Averaging Feedback", IEEE Journal of Solid-State Circuits, vol. 45, no. 6, **(2010)**, pp. 1150-1158.
[15] F. Yuan and N. Soltani, "Low-voltage low V_{DD} sensitivity relaxtion oscillator for passive wireless Microsystems", Electronics Letters, vol. 45, no. 21, **(2009)**, pp. 1057-1058.

Authors

Yong-Rui Zhao, He was born in Hengshui, China, in 1985. He received the B.Sc. degree in electronic & information engineering from Xidian University, Xi' an, China, in 2008. Currently, he is taking a successive postgraduate and doctoral program in circuits & systems in Xidian University. His areas of research include microelectronics, power management and green lighting control. Dr. Zhao has several years of experience in electronic ballast IC and system designing for fluorescent lamps and LED lingting.

Xin-Quan Lai, He was born in Fuping, China, in 1963. He received the B.Sc. degree in Technical Physics and M.Sc. degree in Electronic & Engineering from Xidian University, Xi' an, China, in 1993. And he received the Ph. D. degree in Computer Science & Engineering from the Northwestern Polytechnical University (NPU), Xi' an, China, in 1998. He is currently a professor in Xidian University. His present research interests include mixed signal VLSI/ASIC and SOC design, CMOS sensor, and power management IC design, validation, test and other relative theories.

